JOURNAL

OF THE AMERICAN CHEMICAL SOCIETY

© Copyright 1983 by the American Chemical Society

VOLUME 105, NUMBER 25 DECEMBER 14, 1983

Intramolecular Photochemical Electron Transfer. 1. EPR and Optical Absorption Evidence for Stabilized Charge Separation in Linked Porphyrin–Quinone Molecules[1a]

Alan R. McIntosh,[1b] Aleksander Siemiarczuk,[1b,2] James R. Bolton,*[1b] Martin J. Stillman,*[3] Te-Fu Ho,[1b] and Alan C. Weedon*[1b]

Contribution from the Photochemistry Unit, Department of Chemistry, University of Western Ontario, London, Ontario, Canada N6A 5B7. *Received March 28, 1983*

Abstract: The photochemical properties of diamide-linked porphyrin–quinone molecules (PQ) have been investigated at low temperatures in frozen solvents as a model system for the primary photochemical step of photosynthesis. Electron paramagnetic resonance (EPR) and optical absorption spectroscopies reveal visible light induced changes that are interpreted in terms of intramolecular photochemical electron transfer in the linked porphyrin–quinone molecules. Spin–spin coupling is observed in the EPR spectra, and the light-minus-dark optical difference spectrum produced by irradiation of PQ in 2-methyltetrahydrofuran at 110 K gives evidence of an oxidized porphyrin in the photochemical product complex. Depending on solvent and temperature, about 1–2% of the linked molecules can be converted to a stabilized biradical ion-pair product that is stable for hours at low temperatures. The formation quantum yield of the product species was measured by EPR in several frozen solvents at various temperatures. Evidence is presented that points to the importance of the microviscosity of the solvent matrix in promoting the formation and trapping of the stable intramolecular electron-transfer product.

The primary photochemical step of photosynthesis is a remarkable reaction in that it represents the essential energy-conversion step of sunlight to useful chemical energy. It is now recognized that this primary step involves a one-electron transfer from the excited singlet state of a chlorophyll species to an electron acceptor.[4] This reaction takes place within a reaction-center protein that spans the thylakoid membrane of the chloroplast organelle of green leaves and algae. In reality the reaction-center protein functions as a "solar cell", converting light to electricity, with a photovoltage of ~1.0 V and a solar power-conversion efficiency (at the level of the primary step) of ~16%.[5] The plant then uses this electrical energy to drive the slower biochemical reactions of photosynthesis that ultimately result in the storage of solar energy in plant products such as carbohydrates. By the time storable products are produced, the overall solar-energy storage efficiency of photosynthesis has dropped to ~5% or less.[6]

The photosynthetic reaction-center protein has been well characterized only for bacterial systems,[7] but it is believed that the two reaction-center proteins of green-plant and algal systems have a similar structure to that of the bacterial reaction-center protein.[8] The essential features are as follows: (1) Light absorbed by chlorophyll (or bacteriochlorophyll in photosynthetic bacteria) molecules in an extensive antenna system is channelled, via singlet excitation transfer, to a special (bacterio)chlorophyll center. (2) At this stage part of the photon energy has been converted to the energy of the excited singlet state of the special pigment center. (3) An electron then leaves the (bacterio)chlorophyll center and, residing momentarily on a number of intermediate electron acceptors [which may include (bacterio)chlorophyll, (bacterio)-pheophytin, and iron–sulfur centers], in a time period of a few hundred picoseconds, reaches an electron acceptor. In photosynthetic bacteria, this electron acceptor is a molecule of ubiquinone or menaquinone; in photosystem I of green plants and algae the acceptor is a membrane-bound ferredoxin iron–sulfur

(1) (a) Contribution No. 299, Photochemistry Unit, Department of Chemistry, University of Western Ontario. (b) Photochemistry Unit, The University of Western Ontatio.

(2) Permanent address: Institute of Physical Chemistry, Polish Academy of Sciences, Warsaw, Poland.

(3) Centre for Interdisciplinary Studies in Chemical Physics, The University of Western Ontario.

(4) (a) Katz, J. J.; Norris, J. R.; Shipman, L. L.; Thurnauer, M. C.; Wasielewski, M. R. *Annu. Rev. Biophys. Bioeng.* **1978**, *7*, 393–434; (b) Wasielewski, M. R.; Norris, J. R.; Shipman, L. L.; Lin, C-P.; Svec, W. A. *Proc. Natl. Acad. Sci. U.S.A.* **1981**, *78*, 2957–2961.

(5) The 16% efficiency figure is obtained as follows: for an air mass 1.5 solar spectral distribution, ~36% of the incident solar energy can be converted to excited-state energy at 700 nm. If an average absorption coefficient of 0.9 is assumed, then 32.5% of the incident solar energy will appear as energy of the excited states of the reaction-center chlorophylls. Out of the 1.8-eV excitation energy at 700 nm, ~1.0 eV is generated as electrical energy from the electron-transfer reaction. If we assume a power factor (or curve factor) of 0.9, then the efficiency of the photosynthetic solar cell in the primary electron-transfer step is ~16%.

(6) Bolton, J. R.; Hall, D. O. *Annu. Rev. Energy* **1979**, *4* 353–401.

(7) Feher, G.; Okamura, M. Y. In "The Photosynthetic Bacteria"; Clayton, R. K.; Sistrom, W. R., Eds.; Plenum Press: New York, 1978; pp 349–386.

(8) Thornber, J. P.; Barber, J. In "Topics in Photosynthesis: Photosynthesis in Relation to Model Systems"; Barber, J., Ed.; Elsevier: Amsterdam, 1979; Vol. III, pp 27–70.

0002-7863/83/1505-7215$01.50/0 © 1983 American Chemical Society

center, and in photosystem II the acceptor is a molecule of plastoquinone.[9]

Although simulation in the laboratory of the complete reaction of photosynthesis is an extremely difficult task, it should be possible to simulate or mimic various aspects of the reaction center. Indeed a number of attempts have been made to assemble such biomimetic systems including models of the primary donor and intermediate electron-acceptor complexes,[10] systems incorporated into vesicles, films, and micelles,[11] and model systems involving intramolecular exciplexes.[12]

Since ubiquinone (in bacterial systems) and plastoquinone (in photosystem II of green-plant systems) are involved as electron acceptors in photosynthesis, there has been considerable interest in the study of photochemical electron transfer from chlorophylls or synthetic porphyrins to quinones. Early work involved the study of chlorophyll-sensitized electron transfer to *p*-benzoquinone and its derivatives in organic solvents,[13] where it has been established that the photochemical reaction occurs via the lowest excited triplet state of chlorophyll. Other studies have involved electron transfer to quinones across an interface such as a vesicle.[11c-f,i]

In the past few years a number of groups have synthesized covalently linked porphyrin–quinone molecules in a variety of structures. Kong and Loach[14] in 1978 were the first to report the synthesis of such molecules in their preliminary report of the synthesis of I (Chart I) followed later by a full report.[15] Tabushi et al.[16] reported the synthesis of III and noted that the porphyrin fluorescence was strongly quenched but did not postulate a mechanism. Ganesh and Sanders[17] synthesized a series of quinone-capped metalloporphyrins (IV) (both free base and Mg substituted), of which the UV-visible absorption spectra[17b] show only small differences from normal porphyrins. Ganesh et al.[17c] also report ^{1}H NMR evidence indicating that on average the chromophores are perpendicular and that "this accounts for the relatively unremarkable photochemical properties of these compounds". Nishitani et al.[18] have synthesized a series of octaethylporphyrin–quinone molecules (V) in which M = Zn or H_2 and n = 2, 4, or 6. They found substantial fluorescence quenching in all cases relative to a model octaethylporphyrin and speculated that the quenching was due to intramolecular electron transfer. In a later publication,[19] this group confirmed by picosecond spectroscopy that electron transfer occurs out of the excited singlet state of the porphyrin; they also showed that the lifetime of the charge-transfer state increases, but the rate of the forward reaction decreases with increasing chain length. Netzel et al.[20] have also used picosecond spectroscopy to study the meso-substituted porphyrin–quinone VI synthesized by Dalton and Milgrom.[21] In contrast to the Japanese group[19] they found that in VI the excited singlet state decays primarily to the ground state but also to the triplet state in <6 ps, which then undergoes an electron-transfer reaction. In a later publication, Bergkamp et al.[22] also studied a porphyrin with four quinones in the meso positions and developed a complex kinetic scheme involving a variety of singlet and triplet charge-transfer states. Harriman and Hosie[23] have investigated a number of porphyrins in which a variety of benzene derivatives were introduced symmetrically at the meso positions. They reported fluorescence quantum yields and lifetimes and found strong quenching of fluorescence both in the case of good electron donors (e.g., *N,N*-dimethylaniline) and in the case of good electron acceptors (e.g., *p*-benzoquinone). Lindsey and Mauzerall[24] have reported the synthesis of the cofacial quinone-capped porphyrins VII (M = H_2 or Zn) via entropically favored macropolycyclization. They observed ~60% fluorescence quenching of the zinc-substituted quinone-capped porphyrin relative to the fluorescence yield for a zinc porphyrin lacking the quinone cap, but essentially no quenching in the free-base porphyrin-quinone VII. Finally, Wang et al.[25] have demonstrated that linked porphyrin–quinone molecules incorporated into planar bilayer lipid membranes enhance the photoconductivity and charge separation in these membranes. They reported that the photoelectric effects obtained with these membrane systems are 3 times larger than those of pigmented bilayer membranes containing chlorophyll.

In each of the above studies, only indirect evidence was presented to indicate that electron transfer had indeed occurred following electronic excitation of the porphyrin ring. More conclusive evidence of a stabilized intramolecular electron transfer can be obtained from EPR measurements. Hence, in 1980 we reported[26] an EPR signal from visible-light irradiation of I

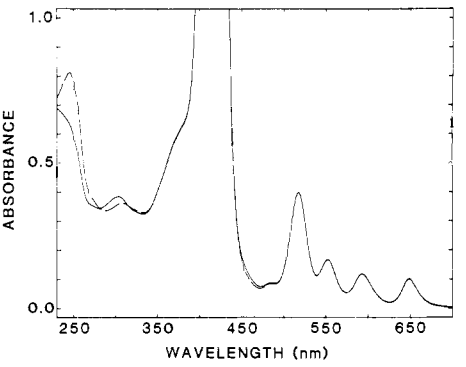

Figure 1. Optical absorption spectra of (PbO_2 oxidized) PA3AQ (——) and untreated II (n = 3) [a 25:75 mixture of PA3AQ and PA3A(QH_2)] (—) in methylene chloride at room temperature.

(9) (a) Bolton, J. R. In ref 7, pp 419–429. (b) Sauer, K. *Annu. Rev. Phys. Chem.* **1979**, *30*, 155–178. (c) Vermaas, W. F. J.; Govindjee *Photochem. Photobiol.* **1981**, *34*, 775–793.

(10) (a) Wasielewski, M. R. In "Frontiers of Biological Energetics—Electrons to Tissues"; Dutton, P. L.; Leigh, J. S.; Scarpa, A., Eds.; Academic Press: New York, 1978; Vol. 1, pp 63–72. (b) Boxer, S. G.; Bucks, R. R. *J. Am. Chem. Soc.* **1979**, *101*, 1883–1885. (c) Pellin, M. J.; Wasielewski, M. R.; Kaufmann, K. J. *Ibid.* **1980**, *102*, 1868–1873.

(11) (a) Ford, W. E.; Otvos, J. W.; Calvin, M. *Proc. Natl. Acad. Sci. U.S.A.* **1979**, *76*, 3590–3593. (b) Kurihara, K.; Sukigara, M.; Toyoshima, Y. *Biochim. Biophys. Acta* **1979**, *547*, 117–126. (c) Pileni, M.-P.; Grätzel, M. *J. Phys. Chem.* **1980**, *84*, 1822–1825. (d) Cheddar, G.; Castelli, F.; Tollin, G. *Photochem. Photobiol.* **1980**, *32*, 71–78. (e) Hurley, J. K.; Castelli, F.; Tollin, G. *Ibid.* **1980**, *32*, 79–86. (f) Shah, S. S.; Holten, D.; Windsor, M. W. *Photobiochem. Photobiophys.* **1980**, *1*, 361–373. (g) Laane, C.; Ford, W. E.; Otvos, J. W.; Calvin, M. *Proc. Natl. Acad. Sci. U.S.A.* **1981**, *78*, 2017–2020. (h) Tunuli, M. S.; Fendler, J. H. *J. Am. Chem. Soc.* **1981**, *103*, 2507–2513. (i) Hurley, J. K.; Castelli,; F., Tollin, G. *Photochem. Photobiol.* **1981**, *34*, 623–631.

(12) (a) Okada, T.; Fujita, T.; Kubota, M.; Masaki, S.; Mataga, N.; Ide, R.; Sakata, Y.; Misumi, S. *Chem. Phys. Lett.* **1972**, *14*, 563–568. (b) Ide, R.; Sakata, Y.; Misui, S. *J. Chem. Soc., Chem. Commun.* **1972**, *1009*. (c) Gnadig, K.; Eisenthal, K. B. *Chem. Phys. Lett.* **1977**, *46*, 339–342. (d) Mataga, N.; Migita, M.; Nishimura, T. *J. Mol. Struc.* **1978**, *47*, 199–219. (e) Migita, M.; Kawai, M.; Mataga, N.; Sakata, Y.; Misumi, S. *Chem. Phys. Lett.* **1978**, *53*, 67–70.

(13) (a) Livingston, R.; Thompson, L.; Ramarao, M. V. *J. Am. Chem. Soc.* **1952**, *74*, 1073–1075. (b) Kelly, J. M.; Porter, G. *Proc. R. Soc. London, Ser. A* **1970**, *A319*, 319–329. (c) Tollin, G. *Bioenergetics* **1974**, *6*, 69–87; *J. Phys. Chem.* **1976**, *80*, 2274–2277. (d) Connolly, J. S.; Gorman, D. S.; Seely, G. R. *Ann. N.Y. Acad. Sci.* **1973**, *206*, 649–669. (e) Holten, D.; Gouterman, M.; Parson, W. W.; Windsor, M. W.; Rockley, M. G. *Photochem. Photobiol.* **1976**, *23*, 415–423. (f) Huppert, D.; Rentzepis, P. M.; Tollin, G. *Biochim. Biophys. Acta* **1976**, *440*, 356–364.

(14) Kong, J. L. Y.; Loach, P. A. In ref 10, pp 73–82.

(15) Kong, J. L. Y.; Loach, P. A. *J. Heterocycl. Chem.* **1980**, *17*, 737–744.

(16) Tabushi, I.; Koga, N.; Yanagita, M. *Tetrahedron Lett.* **1979**, No. 3, 257–260.

(17) (a) Ganesh, K. N.; Sanders, J. K. M. *J. Chem. Soc., Chem. Commun.* **1980**, 1129–1131. (b) Ganesh, K. N.; Sanders, J. K. M. *J. Chem. Soc., Perkin Trans. 1* **1982**, 1611–1615. (c) Ganesh, K. N.; Sanders, J. K. M.; Waterton, J. C. *Ibid.* **1982**, 1617–1624.

(18) Nishitani, S.; Kurata, N.; Sakata, Y.; Misumi, S.; Migita, M.; Okada, T.; Mataga, N. *Tetrahedron Lett.* **1981**, *22*, 2099–2102.

(19) Migita, M.; Okada, T.; Mataga, N.; Nishitani, S.; Kurata, N.; Sakata, Y.; Misumi, S. *Chem. Phys. Lett.* **1981**, *84*, 263–266.

(20) Netzel, T. L.; Bergkamp, M. A.; Chang, C-K.; Dalton, J. *J. Photochem.* **1981**, *17*, 451–460.

(21) Dalton, J.; Milgrom, L. R. *J. Chem. Soc., Chem. Commun.* **1979**, 609–610.

(22) Bergkamp, M. A.; Dalton, J.; Netzel, T. L. *J. Am. Chem. Soc.* **1982**, *104*, 253–259.

(23) Harriman, A.; Hosie, R. J. *J. Photochem.* **1981**, *15*, 163–167.

(24) Lindsey, J. S.; Mauzerall, D. C. *J. Am. Chem. Soc.* **1982**, *104*, 4498–4500.

(25) (a) Wang, C-B.; Tien, H. T.; Lopez, J. R.; Liu, Q-Y.; Joshi, N. B.; Hu, Q-Y. *Photobiochem. Photobiophys.* **1982**, *4*, 177–184. (b) Joshi, N. B.; Lopez, J. R.; Tien, H. T.; Wang, C-B.; Liu, Q-Y. *J. Photochem.* **1982**, *20*, 139–151.

Chart I

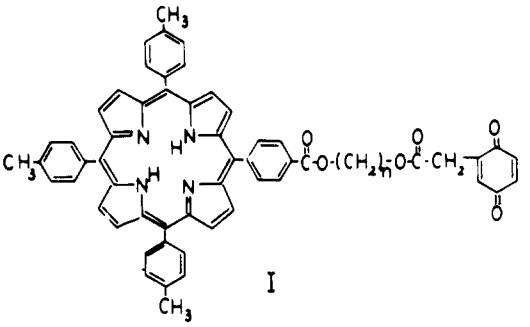

I

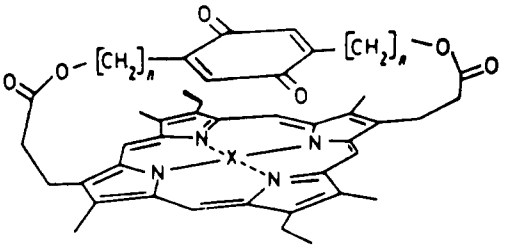

IV

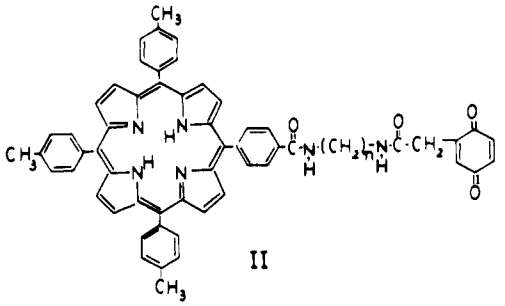

II

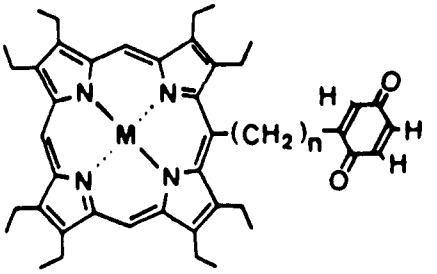

V

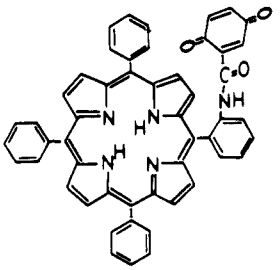

III

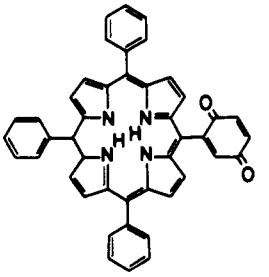

VI

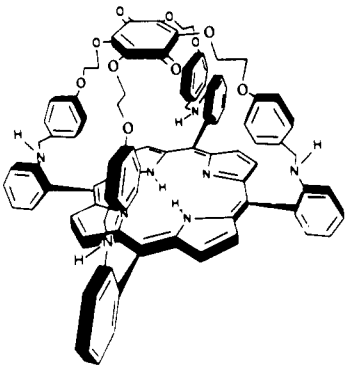

VII

(synthesized by the method of Kong and Loach[15]) at low temperatures which was shown, by a number of control experiments, to arise from intramolecular electron transfer from the porphyrin to the quinone. Under certain conditions this transfer was reversible. Kong and Loach[27,28] have also reported EPR signals from

(26) Ho, T-F.; McIntosh, A. R.; Bolton, J. R. *Nature (London)* **1980**, *286*, 254–256.

(27) Kong, J. L. Y.; Loach, P. A. In "Photochemical Conversion and Storage of Solar Energy"; Connolly, J. S., Ed.; Academic Press: New york, 1981; p 350.

these compounds and the zinc analogues of I.

Connolly[29] has recently published an extensive and comprehensive review of artificial photosynthesis including light-induced electron transfer in chlorophylls and porphyrins, model systems containing chlorophyll dimers and cofacial diporphyrins, and covalently linked porphyrin–quinone complexes.

In this paper we examine the photophysical and photochemical properties of porphyrin–quinone molecules of type II having diamide linkages. We found this linkage to be more stable to hydrolysis than the diester linkage in I. In particular, for these molecules we have concentrated on the photochemical properties observed by EPR and optical absorption spectroscopies in low-temperature, frozen solvent matrices. We have made some measurements with EPR detection in fluid solutions, but at concentrations greater than 10^{-4} M the linked porphyrin–quinone molecules give rise to intermolecular electron transfer, which is not of interest in the present study.

For brevity, we refer to the porphyrin–quinone molecules II with diamide linkages as PA*n*AQ where $n = 2$, 3 or 4. Similarly, we denote the diester-linked molecules I as PE*n*EQ where $n =$ 2, 3, or 4. A and E refer to amide and ester groups, respectively. We have also studied the hydroquinone and dimethoxybenzene derivatives, which we denote by PA*n*A(QH_2) and PA*n*A(DMB), respectively.

Experimental Section

Ho et al.[30a] have synthesized and carried out an extensive characterization of II largely in the hydroquinone form; purity was verified in each case by visible absorption spectrophotometry, ^1H nuclear magnetic resonance (NMR), and mass spectrometry and also by fluorescence techniques. Since the quinone form of these compounds is apparently the photochemically active form, it was necessary to oxidize the hydroquinone to the quinone form. This oxidation was carried out in a heterogeneous mixture by shaking methylene chloride (Fisher spectroscopic grade) solutions ($\sim 10^{-5}$ M) of each compound with excess powdered PbO_2 (Aldrich) at room temperature, followed by filtration through a 10-μm Millipore Teflon filter or a medium-fritted glass filter. The extent of oxidation in samples of II was monitored spectrophotometrically at 246 nm where the quinone moiety shows an absorbance maximum and the hydroquinone form shows markedly lower absorbance. We measured $\epsilon_{248} = 2.03 \times 10^4$ for methyl-*p*-benzoquinone in methylene chloride, which we take as a model for the extinction coefficient for the quinone moiety in the linked porphyrin–quinone compounds. By this assay we found that the product of the organic synthesis was in all cases ($n = 2$, 3, and 4) a mixture of ~25% quinone form and ~75% hydroquinone form. Also by this assay we determined that the $n = 3$ compound could be oxidized to nearly 100% PA3AQ (as shown in Figure 1), whereas the $n = 2$ and 4 compounds could be oxidized only ~75% to PA2AQ and PA4AQ, respectively. For measurements in other solvents, the linked compounds were first oxidized in methylene chloride, evaporated to dryness under a stream of purified nitrogen, and then taken up in the new solvent. The visible absorption spectra were measured in each new solvent to assure that the compounds were still primarily in the quinone form. No metalation of the porphyrin was observed as inferred from unchanged visible absorption spectra in the porphyrin's Soret and Q bands as shown in Figure 1.

The X-band (~9 GHz) EPR measurements were conducted on a Varian E-12 EPR spectrometer equipped with a Varian E-257 temperature controller and interfaced with a Nicolet 2090-III transient recorder and a Nicolet 1180 computer system for the acquisition of steady-state spectra and transient kinetic profiles. A Varian E-9 EPR spectrometer with a low-temperature accessory was utilized for Q-band (~35.5 GHz) measurements. For EPR measurements at X-band solutions of II were transferred to 4-mm o.d. quartz tubes, which were then introduced into the insert dewar of the temperature controller in the EPR cavity which operated in the TM_{110} mode. Q-band measurements were performed in a similar manner on samples in 2-mm o.d. quartz tubes in the insert dewar of the Q-band cavity which operated in the TE_{011} mode.

Table I. Extinction Coefficients (±10%) Measured for PA*n*AQ Compounds in Methylene Chloride at 300 K

	absorption band[a] ($\times 10^{-4}$)				
compd[b]	Soret (B)	Q_y (1,0)	Q_y (0,0)	Q_x (1,0)	Q_x (0,0)
PA2AQ	39 (421)	1.94 (518)	0.82 (553)	0.57 (593)	0.50 (649)
PA3AQ	42 (421)	2.08 (518)	0.85 (553)	0.61 (593)	0.53 (649)
PA4AQ	45 (420)	1.90 (517)	0.99 (551)	0.59 (591)	0.52 (646)

[a] The wavelengths (nm) of the absorption maxima are given in parentheses. [b] 75:25 mixture of PQ and PQH_2 based on UV spectra in the 200–300-nm region. The visible absorption bands change very little on oxidation of PQH_2 to PQ (see text and Figure 1).

The light source for broad-band visible light irradiation was a 150-W tungsten–halogen lamp mounted in a Cole-Parmer Model 9741-50 housing which was furnished with a focussing light pipe to channel the light beam to the EPR cavity. Various Corning cut-off filters and Schott interference filters were employed in series with a 9-cm path-length water filter. Typical light intensities incident on the sample in the EPR cavity were ~10 W m^{-2} after passing through Schott 113 and Corning CS-052 filters and a water filter transmitting $400 < \lambda < 700$ nm.

At X-band the *g* factors of the light-induced EPR spectra were determined by measuring the magnetic-field displacements of the observed spectra from the middle two lines of the six-line EPR spectrum[31] of a solid SrO sample (containing Mn^{2+} as an impurity) which was present in the EPR cavity at the same time as the measurement of the unknown spectrum. Spin concentrations were measured relative to a sample of 4-hydroxy-2,2,6,6-tetramethylpiperidinyl-1-oxy (10^{-3} M) by performing double integrations (with the Nicolet 1180 computer) on the EPR first-derivative spectral data normalized to the same conditions at the same temperature.

Optical absorption measurements were performed on a Hewlett-Packard Model 8450A absorption spectrometer at room temperature and on a Cary Model 219 absorption spectrometer with a 1.00-cm path quartz cell in an Oxford Instruments Model CF204 cryostat operating at 110 K. The linked porphyrin–quinone samples were dissolved in freshly distilled 2-methyltetrahydrofuran (mTHF) (Aldrich), a solvent which forms optically transparent glasses at low temperatures. Samples were changed and allowed to equilibrate thermally while the cryostat was at the operating temperature of 110 K, maintained within ±0.1 K. Irradiations with broad-band visible light were performed with the same tungsten light source that was used in the EPR studies, but filtered through a Corning CS-052 cut-off filter ($\lambda > 400$ nm) or a CS-370 filter ($\lambda > 500$ nm) for some measurements. Optical spectra were digitized directly from the Cary 219 spectrophotometer; the data shown in this paper are computer-drawn plots.[32c] Light-minus-dark optical difference spectra were calculated by computer, and the resulting data were displayed on a Calcomp plotter.

Absolute quantum yields for the formation of the stabilized biradical ion pair $P^+ \cdot Q^- \cdot$, which results from the intramolecular electron-transfer reaction from the porphyrin (P) to the quinone (Q), were determined under a variety of conditions by employing a variation of the method described by Chew and Bolton.[33] The quantum yield of formation of stabilized $P^+ \cdot Q^- \cdot$ was taken as one half of the quantum yield of the generated $P^+ \cdot Q^- \cdot$ spin concentration formation. We measured the rate of increase of the light-induced EPR signal relative to the response observed from a sample of photosystem I enriched subchloroplast particles (from spinach) prepared by the method of Vernon and Shaw.[34] The light source for the absolute quantum-yield measurements was a Spectra-Physics Model 164-01 CW krypton ion laser operating at 647 nm and at relatively low power outputs (<40 mW) to preclude melting of the frozen samples through thermal dissipation of localized light absorption. Relative quantum yields as a function of temperature were carried out at ~10 W m^{-2} with the tungsten lamp described earlier filtered through

(28) (a) Kong, J. L. Y.; Spears, K. G.; Loach, P. A. *Photochem. Photobiol.* **1982**, *35*, 545–553. (b) Loach, P. A.; Runquist, J. A.; Kong, J. L. Y.; Dannhauser, T. J.; Spears, K. G. In "Electrochemical and Spectrochemical Studies of Biological Redox Components"; Kadish, K. M., Ed.; American Chemical Society: Washington, DC, 1982; ACS Symp. Ser. No. 201, pp 515–561.

(29) Connolly, J. S. In "Photochemical Conversion and Storage of Solar Energy—1982"; Rabani, J., Ed.; The Weizmann Science Press of Israel: Jerusalem, 1982; Part A, pp 175–204.

(30) (a) Ho, T-F.; McIntosh, A. R.; Weedon, A. C. *Can. J. Chem.*, submitted for publication. (b) Siemiarczuk, A.; McIntosh, A. R.; Ho, T-F.; Stillman, M. J.; Roach, K. J.; Weedon, A. C.; Bolton, J. R.; Connolly, J. S. *J. Am. Chem. Soc.*, following paper in this issue.

(31) Bolton, J. R.; Borg, D. C.; Swartz, H. M. In "Biological Applications of Electron Spin Resonance"; Swartz, H. M.; Bolton, J. R.; Borg, D. C., Eds.; Wiley-Interscience: New York, 1972; p 100.

(32) (a) Fajer, J.; Borg, D. C.; Forman, A.; Dolphin, D.; Felton, R. H. *J. Am. Chem. Soc.* **1970**, *92*, 3451–3459. (b) Dolphin, D.; Muljiani, Z.; Rousseau, K.; Borg, D. C.; Fajer, J.; Felton, R. H. *Ann. N.Y. Acad. Sci.* **1973**, *206*, 177–200. (c) Browett, W. R.; Stillman, M. J. *Inorg. Chim. Acta* **1981**, *49*, 69–77.

(33) Chew, V. S. F.; Bolton, J. R. *J. Phys. Chem.* **1980**, *84*, 1903–1908.

(34) Vernon, L. P.; Shaw, E. R. In "Methods in Enzymology" San Pietro, A., Ed.; Academic Press: New York, 1971; Vol. 23, pp 277–289.

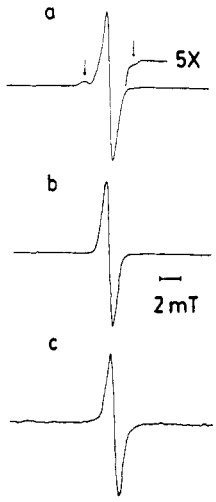

Figure 2. Light-induced EPR spectra observed from irradiations of the linked porphyrin–quinone compounds II, each in frozen methylene chloride, after irradiation at 140 K with a broad-band visible light ($400 < \lambda < 700$ nm) at ~ 10 W m^{-2} for ~ 30 min. EPR conditions: modulation amplitude, 0.2 mT; microwave power, 1 mW at 8.97 GHz (X-band); 16 scans averaged for each spectrum. The crossover point in each spectrum corresponds to a g factor of 2.0037 ± 0.0002. (a) 3×10^{-4} M PA2AQ. (b) 3×10^{-4} M PA3AQ. (c) 2×10^{-4} M PA4AQ.

a Corning CS-052 filter transmitting from 400 to 700 nm. For all the quantum-yield measurements the concentrations were adjusted so that the absorbances at 647 nm were ~0.3 in the 2-mm path length of the quartz EPR tubes at room temperature. For the linked porphyrin–quinone systems, this corresponds to concentrations of $\sim 3 \times 10^{-4}$ M as determined from independent measurements[30a] of the extinction coefficients in methylene chloride; these data are presented in Table I. Any of the molecules II in the hydroquinone form (~25% for PA2AQ and PA4AQ) were considered to be photochemically inactive[30b] when the relative quantum yields were calculated.

We measured the quantum yield for formation of $P700^+$ in the subchloroplast standard sample in a glassy 1:1 glycerol–water solid matrix at 135 K and found it to be 0.75, which is in agreement with a previously measured value.[35] Neutral-density filters were employed to reduce the incident laser power by at least a factor of 100 so that the rate of P700 oxidation in the subchloroplast samples was retarded to the point where the rate of the EPR signal rise was comparable to the growth of the EPR signal in the linked porphyrin–quinone samples under otherwise identical conditions of light absorption and temperature. Thus valid comparisons could be made between the relatively high quantum yield seen in subchloroplast samples and the much lower quantum yields of the linked porphyrin–quinone samples. The respective first-derivative EPR spectra were twice integrated by computer; hence the relative quantum yields were determined directly in terms of the relative rates of change of spin concentrations.

Results

1. EPR Measurements. We have conducted EPR measurements with visible light irradiation at low temperatures of the PA*n*AQ (n = 2–4) compounds for concentrations between 10^{-5} and 10^{-3} M in the following frozen solvents: 95:5 methanol/water, 95:5 ethanol/water, 1-propanol, 2-propanol, 1-butanol, 2-methyltetrahydrofuran (mTHF), chloroform, methylene chloride, 1:1 methanol/glycerol, and 5:5:2 EPA (diethyl ether/isopentane/ethanol). In all cases, irradiation of the PQ molecules with broad-band ($400 < \lambda < 700$ nm) visible light or with red light for temperatures between 100 and 150 K in these frozen matrices results in the appearance of EPR signals of $g = 2.0037 \pm 0.0002$. The peak-to-peak line width (ΔH_{pp}) for PA2AQ varies from 0.88 to 1.05 mT, depending on the solvent and temperature. However, under identical conditions the EPR spectra formed from PA3AQ or PA4AQ are ~0.05 mT narrower than for PA2AQ.

Typical light-induced EPR spectra for all three PA*n*AQ molecules are shown in Figure 2. These EPR signals develop after several minutes of irradiation, attaining a maximum value after ~20 min. The signals are formed essentially irreversibly, exhibiting a slow partial decay over minutes to hours after cessation of the irradiation. This is in contrast to the mostly reversible EPR signals observed from the diester linked compound PE3EQ in a frozen methanol matrix at ~160 K.[26]

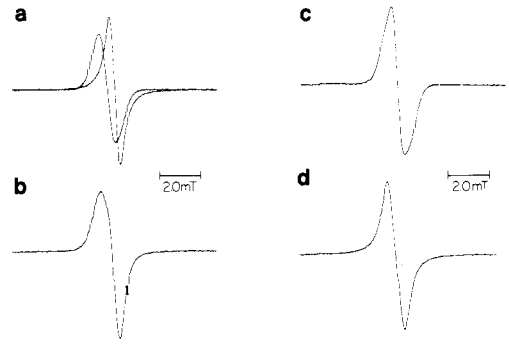

Figure 3. EPR spectra observed at 140 K with modulation amplitude 0.2 mT; microwave power 1 mW at 8.97 GHz (X-band). (a) Superposition of $P^{+\cdot}$ (obtained from the Br_2 oxidation of tetratolylporphyrin in methylene chloride) with $\Delta H_{pp} = 0.55$ mT and $g = 2.0025$ and of $Q^{-\cdot}$ (obtained from the air oxidation of 2-methylhydroquinone in methanol) with $\Delta H_{pp} = 0.8$ mT and $g = 2.0047$. Each spectrum corresponds to the same concentration of radicals (i.e., the double integrals are the same). (b) Digital addition of the spectra of $P^{+\cdot}$ and $Q^{-\cdot}$ from (a). The crossover point has $g = 2.0032 \pm 0.0002$. (c) Experimental spectrum obtained from the visible light photolysis at 150 K of 5×10^{-4} M tetratolylporphyrin mixed with 5×10^{-2} M 2-methylquinone in methylene chloride followed by cooling to 140 K. The crossover point has $g = 2.0032 \pm 0.0002$. (d) Simulated spectrum of $P^{+\cdot}Q^{-\cdot}$ with $\Delta g = 0.35$ mT and $J = 0.15$ mT. The crossover point has $g = 2.0037$.

We have carried out a number of control experiments to ascertain the identity of these EPR signals. These control experiments are very important because a variety of artifactual sources for the EPR signals are possible.

(a) What chromophore is responsible for the EPR signals? Experiments conducted with interference filters clearly establish that only visible wavelengths specifically absorbed by the porphyrin chromophore are active in generating the EPR signals.

(b) Is the covalent linkage between P and Q important? To test this question solutions were made up containing equimolar amounts of tetratolylporphin (P) and 2-methylquinone (Q) at the same concentration as used for the experiments with the linked PQ compounds. No light-induced EPR signals could be generated. The negative result in this control indicates that the EPR signals do not arise from intermolecular electron transfer between isolated P and Q molecules.

(c) Can the EPR spectrum be explained in terms of a simple superposition of EPR spectra of $P^{+\cdot}$ and $Q^{-\cdot}$? By treating tetratolylporphyrin with Br_2 in methylene chloride it was possible to oxidize P to $P^{+\cdot}$; similarly, by air oxidation of 2-methylhydroquinone in methanol it was possible to generate the $Q^{-\cdot}$ radical anion. These two EPR spectra are shown superimposed in Figure 3a where the amplitudes of each have been adjusted so that the two spectra represent equimolar amounts of $P^{+\cdot}$ and $Q^{-\cdot}$. In Figure 3b we show the digital addition of the two spectra in Figure 3a. In Figure 3c we show the EPR spectrum obtained when a frozen mixture of $\sim 5 \times 10^{-4}$ M tetratolylporphyrin and 100 times excess ($\sim 5 \times 10^{-2}$ M) of 2-methylquinone in methylene chloride is irradiated with visible light 10 K below the melting point of the solvent. Presumably in this case $P^{+\cdot}$ and $Q^{-\cdot}$ are being formed in equimolar amounts by intermolecular electron transfer resulting in isolated $P^{+\cdot}$ and $Q^{-\cdot}$ molecules. Clearly the composite spectrum in Figure 3b is very similar to that in Figure 3c. In both cases the spectra are slightly asymmetric with a crossover point that corresponds to a g factor of 2.0032 ± 0.0002; $\Delta H_{pp} = 0.90 \pm 0.02$ mT. On the basis of the agreement between the spectra in Figure 3, parts b and c, we assign the spectrum in Figure 3c to an equimolar mixture of isolated $P^{+\cdot}$ and $Q^{-\cdot}$ molecules.

A careful comparison of the EPR spectra in Figure 2 with those of Figure 3, part b or c, reveals that there are two distinct, reproducible differences. The spectra in Figure 2 are quite sym-

(35) Borisov, A. Yu.; Il'ina, M. D. *Biochim. Biophys. Acta* **1973**, *325*, 240–246.

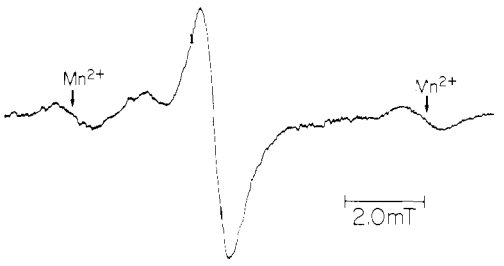

Figure 4. Q-band EPR spectrum observed from the irradiation of PA2AQ at 5×10^{-4} M in methylene chloride at 140 K. EPR conditions: modulation amplitude, 0.5 mT; microwave power, 30 dB down from 50 mW at 35.5 GHz. The two partially resolved lines due to $P^{+}\cdot Q^{-}\cdot$ are seen between the Mn^{2+} lines (marked by arrows) observed from the quartz tubes used to contain the samples.

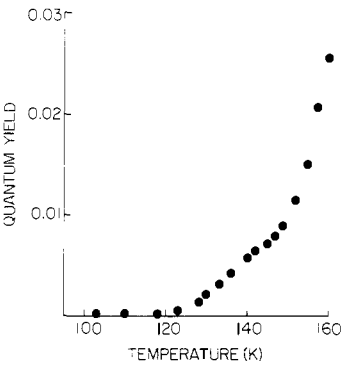

Figure 5. Temperature dependence of the quantum yield for formation of $P^{+}\cdot Q^{-}\cdot$ from PA3AQ as measured by EPR in a 95:5 methanol:water matrix.

metric, in contrast to the asymmetry exhibited in the spectra in Figure 3b,c, and the g factor for the spectra in Figure 2 is 0.0005 unit higher than the g factor for the spectra in Figure 3b,c. Furthermore, the EPR spectrum of PA2AQ in Figure 2a exhibits broad satellites ~20 G above and below the center peak. Clearly, the EPR spectra in Figure 2 cannot be explained in terms of a simple superposition of the EPR spectra of isolated $P^{+}\cdot$ and $Q^{-}\cdot$ molecules. We believe that the differences found between the EPR spectra arise from an intramolecular interaction between the two radical ions in a linked $P^{+}\cdot Q^{-}\cdot$ biradical ion pair.

(d) Is the presence of a linked quinone important for the formation of the EPR signals? Irradiation of frozen solutions of PA*n*A(DMB) compounds (where the quinone moiety has been replaced by a dimethoxybenzene moiety) results in the observation of negligibly small (about 100-fold weaker) EPR signals in a variety of solvents. Furthermore, it was found that reduction of PA3AQ to PA3A(QH_2) with KBH_4 in ethanol resulted in a photochemically inactive sample. Finally, oxidation of untreated II (~25% PA3AQ) with solid PbO_2 resulted in greatly enhanced EPR signals. All of this evidence indicates that the presence of the quinone electron-acceptor moiety in the linked compounds is essential for the generation of the EPR signals.

The above control experiments clearly demonstrate that the EPR signals in Figure 2 must be assigned to the formation of the linked $P^{+}\cdot Q^{-}\cdot$ radical-ion pair in which there is some interaction between the unpaired electrons in the two radical ions. Two types of interaction are possible: electron–spin exchange coupling and dipolar coupling.[36] For two radicals with nearly the same g factors, it is well-known that if the magnetic field difference due to the difference in g factors is comparable to or slightly greater than $hJ/g\beta$, where h is Planck's constant, β is the Bohr magneton, and J is the electron spin exchange coupling constant (Hz), the EPR spectrum should consist of two relatively strong, closely spaced inner lines and two weaker outer lines all centered at the average g factor of the two radicals.[36,37] This pattern is analogous to the AB quartet arising from the strong coupling of two proton spins in NMR.[38] We interpret our light-induced X-band EPR spectra in Figure 2 for all the PA*n*AQ molecules as an unresolved spin-exchange pattern with J between 0.1 and 0.2 mT. At the X-band frequency (~9.0 GHz), we observe a magnetic field difference of 0.35 mT between the isolated EPR spectra of $P^{+}\cdot$ and $Q^{-}\cdot$ in Figure 3a. The g factor for $P^{+}\cdot$ is $g = 2.0025$,[26] and the apparent g factor for $Q^{-}\cdot$ is $g = 2.0047$ at X-band which is the average of the unresolved g and hyperfine anisotropy.[39] Thus, for spin exchange between $P^{+}\cdot$ and $Q^{-}\cdot$, the above condition of very similar g factors is met. Indeed the g factor observed for $P^{+}\cdot Q^{-}\cdot$ from the PA*n*AQ molecules is very close to the average of the g factors of isolated $P^{+}\cdot$ and $Q^{-}\cdot$ radical ions. In Figure 3d, we present a simulated isotropic spin exchange spectrum for $P^{+}\cdot Q^{-}\cdot$ where $\Delta g = 0.35$ mT and $J = 0.15$ mT, and it is observed to have the g factor, line width, and relative symmetry of the PA*n*AQ spectra of Figure 2b,c. (We return to Figure 2a later.)

Further evidence of a small but significant value of J was obtained by performing Q-band (~35.5 GHz) EPR measurements. The low-temperature Q-band spectrum (shown in Figure 4) reveals a partially resolved pair of lines at g factors close to those expected for individual $P^{+}\cdot$ and $Q^{-}\cdot$ components. In this case the lines are separated by the field difference ~1.4 mT, which is to be compared with the 1.75 mT difference corresponding to the difference in g of $P^{+}\cdot$ and g^{yy} of $Q^{-}\cdot$ at 35.5 GHz. (The expected g factor anisotropy[39] of $g^{xx} = 2.0065$, $g^{yy} = 2.0053$, and $g^{zz} = 2.0023$ of $Q^{-}\cdot$ was not well resolved in our nondeuterated Q-band EPR spectra.) The magnetic field and frequency are both ~4 times larger at Q band; now J (0.1–0.2 mT) is much less than the field difference arising from the different g factors, and hence the individual spectra of $P^{+}\cdot$ and $Q^{-}\cdot$ are partially resolved.

The EPR spectrum of $P^{+}\cdot Q^{-}\cdot$ from PA2AQ (shown in Figure 2a) is broader than those of PA3AQ or PA4AQ and also exhibits broad, weak satellites. The broader line width can be explained in terms of a slightly larger value of J, consistent with the shorter chain length. However, we ascribe the satellites to a dipolar coupling arising from a subset of the $P^{+}\cdot Q^{-}\cdot$ molecules in which the $P^{+}\cdot$ and $Q^{-}\cdot$ moieties are close enough to interact with each other.

As shown in paper 2,[30b] there are at least two families of conformations present in all of the PA*n*AQ molecules, a "complexed" set of conformers in which the porphyrin and quinone entities are close enough to interact electronically to show optical line broadening and an "extended" set of conformers in which the porphyrin and quinone are far enough apart so that they do not interact. We believe that the dipolar coupling in the PA2AQ case arises from the complexed conformers, while the center line arises mainly from the extended conformers. The magnitude of the dipolar splitting (~2.0 mT) allows us to estimate an average separation of 10–12 Å between the two unpaired electrons. Molecular models show that this center-to-center distance is consistent with a folded conformation in which the quinone interacts with the nearest phenyl in the linking chain, but this distance is not consistent with extended conformations.

We observe evidence of spin-exchange coupling in all three of the PA*n*AQ molecules, although J seems to be slightly larger in PA2AQ. This is reasonable since J depends upon orbital overlap and is proportional to r^{-1}; also there is only a slight increase in the average distance between $P^{+}\cdot$ and $Q^{-}\cdot$ as n is increased due to the flexibility of the chain. However, the dipolar coupling falls off as r^{-6}; hence it is reasonable that dipolar coupling can be observed only for the shortest chain length.

2. Quantum-Yield Measurements. Quantum yields for the appearance of the stabilized $P^{+}\cdot Q^{-}\cdot$ species were measured by EPR relative to the yield of photochemical oxidation of P700 in photosystem I enriched subchloroplast particles as described in the Experimental Section. The quantum yields were found to vary with temperature,[40] as shown in Figure 5 for a glassy 95:5

(36) Schepler, K. L.; Dunham, W. R.; Sands, R. H.; Fee, J. A.; Abeles, R. H. *Biochim. Biophys. Acta* **1975**, *397*, 510–518.
(37) Prince, R. C.; Tiede, D. M.; Thornber, J. P.; Dutton, P. L. *Biochim. Biophys. Acta* **1977**, *462*, 467–490.
(38) Pople, J. A.; Schneider, W. G.; Bernstein, H. J. "High Resolution Nuclear Magnetic Resonance"; McGraw-Hill: New York, 1959; p 122.
(39) (a) Hales, B. J. *J. Am. Chem. Soc.* **1975**, *97*, 5993–5997. (b) Hales, B. J.; Das Gupta, A. *Biochim. Biophys. Acta* **1979**, *548*, 276–286.

Table II. Quantum Yields for Formation of Stabilized $P^+ \cdot Q \cdot$ Measured 20 and 40 K below Each Solvent's Softening Point

compd	solvent	softening point (T_s), K	quantum yield (±10%) $T_s - 40$ K	$T_s - 20$ K
PA2AQ	CH_2Cl_2	178	0.0044	0.026
PA3AQ	CH_2Cl_2	178	0.0042	0.028
PA4AQ	CH_2Cl_2	178	0.0003	0.003
PA2AQ	95:5 CH_3OH/H_2O	180	0.0062	0.022
PA3AQ	95:5 CH_3OH/H_2O	180	0.0057	0.024
PA4AQ	95:5 CH_3OH/H_2O	180	0.0004	0.004
PA2AQ	95:5 C_2H_5OH/H_2O	155	0.0039	0.016
PA3AQ	95:5 C_2H_5OH/H_2O	155	0.0026	0.013
PA4AQ	95:5 C_2H_5OH/H_2O	155	0.0002	0.002
PA2AQ	1-propanol	145	<0.0001	0.005
PA3AQ	1-propanol	145	<0.0001	0.005
PA4AQ	1-propanol	145	<0.0001	0.0005
PA2AQ	1-butanol	185	<0.0001	0.001
PA3AQ	1-butanol	185	<0.0001	0.001
PA4AQ	1-butanol	185	<0.0001	<0.0001
PA2AQ	mTHF	130	0.0018	0.009
PA3AQ	mTHF	130	0.0013	0.006
PA4AQ	mTHF	130	<0.0001	<0.0001

methanol/water solvent matrix. It is clear that the quantum yields increase dramatically ~20 K below the softening point of the solvent matrix. A similar temperature dependence was found for all solvent systems studied, and in each case the maximum quantum yield, which could be measured practically by EPR (without partially melting the samples), was close to ~20 K below the melting or softening point of each solvent matrix system; these quantum yields are listed in Table II along with a set taken at ~40 K below the respective softening points for comparison. It can be seen from these data that the highest quantum yield for production of $P^+ \cdot Q^- \cdot$ was obtained in methylene chloride even though this solvent does not form a glassy solvent matrix. In our measurements we measure the quantum yield of *stabilized* $P^+ \cdot Q^- \cdot$; however, we anticipate that the transient yield of $P^+ \cdot Q^- \cdot$ will probably be much higher in all solvents.

As the temperature is raised to the melting point and higher, EPR spectra could be observed in several solvents when the concentration of the PQ molecules was $\geq 10^{-4}$ M. These spectra exhibit hyperfine structure characteristic of a relatively stable radical anion, which can be assigned to the semiquinone moiety of the PQ molecule. We believe that these EPR signals arise from *inter*molecular electron transfer since similar EPR spectra were observed on irradiation of equimolar concentrations of the unlinked porphyrin and quinone in solutions at these same higher temperatures. These extraneous EPR spectra interfered with measurements of formation quantum yields of $P^+ \cdot Q^- \cdot$ at temperatures close to the respective melting points of each solvent system; hence, we were not able to measure quantum yields under these conditions.

We also measured the total yield, i.e., the maximum fraction of PQ which could be converted to $P^+ \cdot Q^- \cdot$ after prolonged steady-state irradiation with broad-band visible light. We found that in most of the previously mentioned solvents this yield was remarkably similar (usually ~1% at temperatures ~20 K below the melting point of each solvent), even for those solvents with low quantum yields. The exceptions were methanol and methylene chloride in which it was possible to obtain ~2% conversion to $P^+ \cdot Q^- \cdot$.

3. Optical Measurements. We have confirmed that the linked PQ compounds follow Beer's law in methylene chloride, ethanol, and mTHF over a concentration range of $\sim 1 \times 10^{-6}$ to $\sim 2 \times 10^{-3}$ M, the latter being the solubility limit for PA2AQ; for PA4AQ in methylene chloride Beer's law behavior could be confirmed only up to its solubility limit, 5×10^{-4} M. The fact that Beer's law holds over such large concentration ranges indicates that oligomer formation is negligible in the solvents tested, even at moderately high concentrations.[41]

We have measured the optical absorption changes that occur in PA2AQ and PA3AQ solutions when irradiated at 110 K with broad-band visible light at light intensities of ~10 W m^{-2}. The sample concentrations were typically between $\sim 2 \times 10^{-6}$ M and $\sim 6 \times 10^{-5}$ M in mTHF; the glassy samples were contained in a 1.00-cm-path square quartz cell in a cryostat maintained at 110 K (±0.1 K) inside the Cary Model 219 spectrophotometer. Typical optical absorption and light-minus-dark difference spectra for PA3AQ are shown in Figure 6. The most prominent feature is a strong, light-induced positive absorbance change with a maximum at 478 nm and also a weaker broad absorption with maxima near 680 nm and 725 nm. These spectral changes were found to be very stable in the dark as judged by spectra recorded at 110 K for as long as 1 h after irradiation. This behavior parallels that found for the light-induced EPR spectra at 110 K in mTHF. The optical difference spectrum in Figure 6c exhibits an apparent first-derivative line shape at the position of some of the absorption bands. This behavior can be interpreted as a conformational change (or photoisomerization) of the PQ molecules[30b] during irradiation at 110 K; however, the unlinked tetratolylporphyrin itself does not exhibit such spectral shifts on irradiation. Note that the optical difference spectra of Figure 6c,d are positive nearly everywhere, which shows that the spectrum of the photochemical product comprises broad bands with reasonably high absorbance relative to the ground-state porphyrin, outside the Q and Soret band regions of the unoxidized porphyrin. It is clear that in the optical difference spectra of Figure 6c,d new absorption bands appear, particularly in the 700-nm region. This means that a species is being formed with absorption well to the red of the $Q_x(0,0)$ band of the porphyrin. Similar optical spectra were measured for PA2AQ samples in mTHF at 110 K.

We attempted to measure optical difference spectra of PA4AQ under the same conditions, but no light-induced changes in the Q bands were observed; this is consistent with the low quantum yields measured by EPR for this compound (see Table II). We also attempted to measure optical difference spectra for linked PQ compounds with $n = 2$ and 3 where the quinone was replaced by a dimethoxybenzene moiety (a precursor in the organic syntheses[30a]). Depending on the sample history, either red-shifted or blue-shifted changes in the Soret and Q bands could be produced by irradiation of the PA2A(DMB) and PA3A(DMB) samples under the same conditions at 110 K. This is further evidence that these spectral shifts are due to a photoisomerization process occurring during low-temperature irradiation of these linked molecules.[30b]

Discussion and Conclusions

We believe that our analysis of the EPR signals from the visible-light irradiation of PA*n*AQ molecules provides strong evidence that the EPR signals arise from intramolecular electron transfer to produce the biradical ion pair $P^+ \cdot Q^- \cdot$.

The question can be raised as to whether or not an observed spin exchange effect has any connection with the rate of back electron transfer. In bacterial reaction centers, a value of J = 6.0 mT has been measured[37] under a variety of conditions for the exchange coupling between the reduced "primary" acceptor pheophytin and the reduced secondary acceptor ubiquinone. Presumably the electron back reaction in nonreduced reaction centers back to the oxidized donor $P870^+$ follows the same path as in the forward reaction, that is, through the pheophytin. The rate of this back reaction[7] is ~50 s^{-1} compared to the electron "exchange" rate of ~10^8 s^{-1}. Clearly in this case there is no direct connection, nor do we believe there is any connection in our case. This is, however, an interesting theoretical problem.

(40) These are relative quantum yields measured by EPR where the Curie law $1/T$ dependence of the EPR signal intensities has been taken into account.

(41) Without independent measurements of molecular weight, dimer formation cannot be ruled out unabmiguously. However, it would then be necessary to postulate that all these porphyrin systems are dimeric even at concentrations as low as ~10^{-6} M. On the basis of the observed absorption spectra (e.g., Figure 6), such a postulate does not seem tenable to us.[42]

(42) White W. I. In "The Porphyrins"; Dolphin, D., Ed.; Academic Press; New York, 1978; Vol. V, pp 303–339.

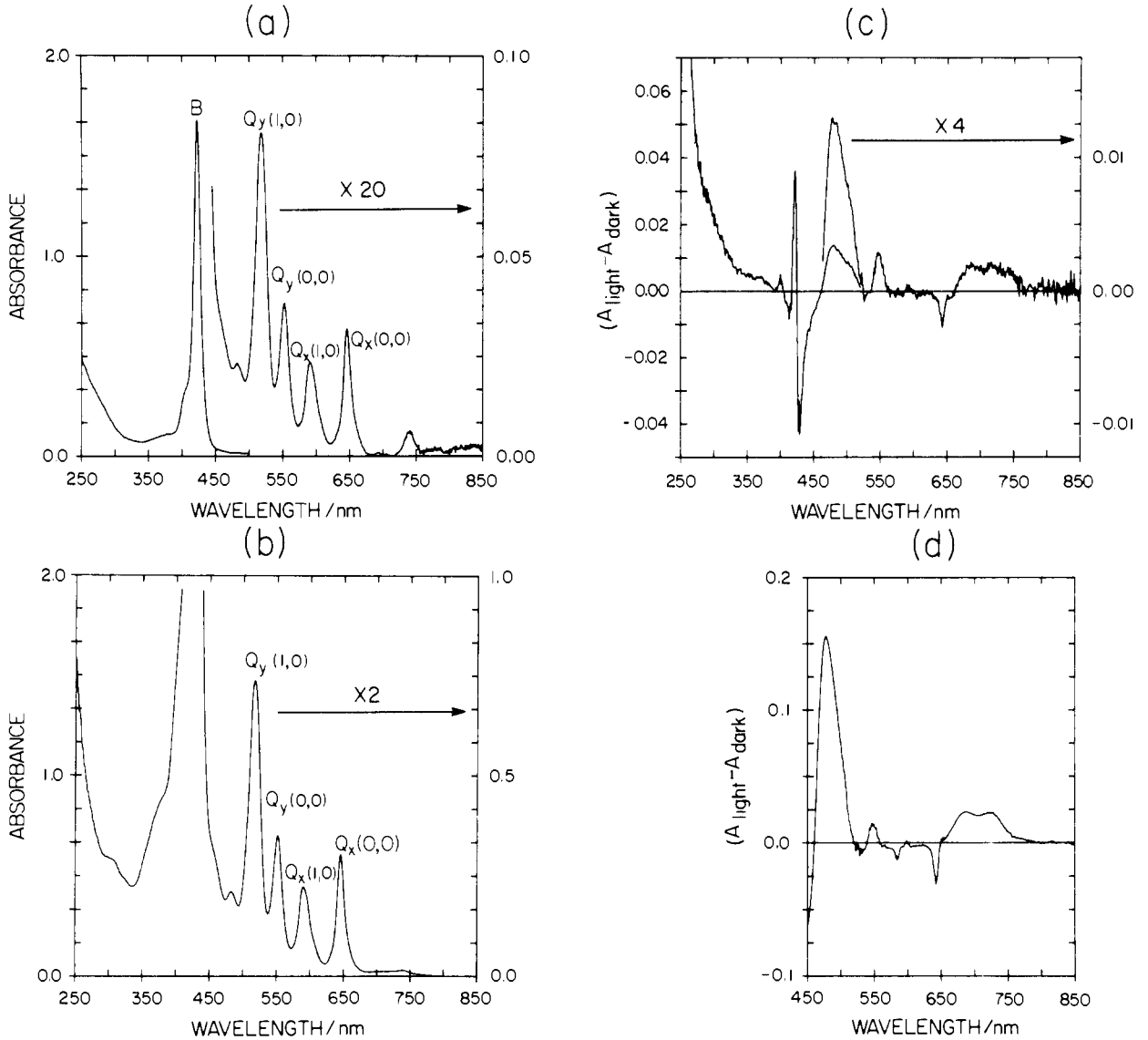

Figure 6. Optical absorption spectra of PA3AQ dissolved in mTHF at 110 K: (a) Absorption spectrum of $\sim 4 \times 10^{-6}$ M PA3AQ. The very weak absorption at ~730 nm is due to the solvent. The absorbance scale for the Soret (B) band is 0–2 and for the Q bands is 0–0.1. (b) Absorption spectrum of $\sim 4 \times 10^{-5}$ M PA3AQ. Intensification of the $Q_x(0,0)$ band relative to the $Q_x(1,0)$ band occurs gradually as the temperature is lowered from 300 to 110 K. The same relative intensities are present in the spectrum of the more dilute sample shown in (a). (c) Optical difference spectrum (light-minus-dark) of 4×10^{-6} M PA3AQ as in (a) after irradiation with visible light with $\lambda > 400$ nm at 110 K at 10 W m^{-2} for 30 min. (d) Optical difference spectrum of 4×10^{-5} M PA3AQ in (b) under the same conditions as (c) to show more detail in the Q-band region.

The EPR measurements at low temperature indicate that only ~1–2% of the PQ molecules can be converted to the stable (for hours) $P^+ \cdot Q^- \cdot$ state. Both the total yield and the quantum yield of $P^+ \cdot Q^- \cdot$ formation increase sharply in the solid state ~20 K below the melting point of any given solvent system. This behavior points to the importance of the relative microviscosity of the solid matrix to allow trapping of the $P^+ \cdot Q^- \cdot$ state. One interpretation is that, even at these low temperatures, some torsional mobility of the P and Q moieties is maintained and provides vibronic "fine-tuning" of the forward electron transfer and subsequent trapping of the $P^+ \cdot Q^- \cdot$ state. This interpretation is reinforced by the fluorescence behavior of these molecules.[30b]

There is no obvious dependence on solvent dielectric constant or polarity of the formation quantum yields of stable $P^+ \cdot Q^- \cdot$ at low temperatures. However, we observed that the quantum yield of $P^+ \cdot Q^- \cdot$ production was much less in 1-propanol and 1-butanol (the longest chain alcohols employed as solvent matrices) than in the other matrices. The dielectric constants of alkyl alcohols decrease with chain length[43] (from $\epsilon = 54$ at 200 K for methanol to $\epsilon = 38$ at 200 K for 1-propanol); however, it seems unlikely that such a small change in dielectric constant could be responsible for the dramatic decrease in quantum yield of the $P^+ \cdot Q^- \cdot$ photoproduct. We suggest that the observed decrease in quantum yields is caused by an increase in the microviscosity of the solvent medium (even at 40 K below the melting point) as the alcohol chain length is increased from methanol to 1-butanol.

There does, however, appear to be some dependence of the formation quantum yield of stable $P^+ \cdot Q^- \cdot$ on the length of the molecular chain linking the porphyrin and quinone. Thus PA4AQ has a significantly lower quantum yield than either PA2AQ or PA3AQ. These observations suggest that the linkage in PA4AQ is beyond a critical length where it can be locked into conformations that are relatively favorable for efficient transfer of an electron from the porphyrin to the quinone.

If the assignment of the observed EPR spectra to $P^+ \cdot Q^- \cdot$ radical pairs is correct, then we should be able to observe the corresponding optical spectrum following irradiation at low temperature. The spectra of porphyrin radical cations are known to be distinctive,[32] and large changes in absorption are to be expected if a porphyrin radical cation is formed. The light-induced optical difference spectra in PA2AQ and PA3AQ prove that in each case

(43) Weast, R. C., Ed. "Handbook of Chemistry and Physics"; CRC Press: Cleveland, 1976; Vol. 56, p E-56.

the π-electron distribution in the porphyrin moiety has changed following irradiation in mTHF. To the best of our knowledge, an absorption spectrum for a singly oxidized metal-free D_{2h} tetraphenyl- or tetratolylporphyrin (i.e., $P^{+}\cdot$) has not been reported previously. One report[44a] of such a spectrum does not appear to be correct, but rather has the features of a D_{4h} protonated porphyrin dication which has distinctive spectral properties when observed under acidic conditions.[44b] The generation of $P^{+}\cdot$ optical spectra for free-base tetraphenylporphyrins is not easy as the compounds are very difficult to oxidize. Very recently we have obtained the spectrum[44c] of singly oxidized TPP by photolysis of TPP at 77 K; the absorption data do exhibit bands in the regions of positive growth in the difference spectra shown in Figure 6d for PQ. The quantum yield for formation of the oxidized $TPP^{+}\cdot$ was about 0.02.

The observed difference spectrum shown in Figure 6d appears to be dominated by a strongly absorbing $P^{+}\cdot$ entity that has characteristic absorption peaks at ~478 nm and two overlapping peaks at 680 and 725 nm; these features are similar to those observed[32] in singly oxidized metalloporphyrins. The radical anion of methyl-*p*-benzoquinone would be expected to show a positive absorbance change in the region of 300–450 nm.[45,46] An attempt was made to add back the "dark" spectra to the observed light-minus-dark spectra so as to obtain pure $P^{+}\cdot Q^{-}\cdot$ spectra. This was not totally successful due to the assumed photoisomerization spectral changes mentioned earlier. Nevertheless, we can conclude that the fractional conversion to $P^{+}\cdot Q^{-}\cdot$ was ~1%, in agreement with the EPR determination of the total yield of $P^{+}\cdot Q^{-}\cdot$ in mTHF at 110 K.

Although the quantum yields we have obtained are much smaller than those found in vivo (where electron-transfer quantum yields approaching unity are observed[47]), it is significant that our model compounds show appreciable stable-product yields of ~1%. We found that the quantum yields for production of stabilized $P^{+}\cdot Q^{-}\cdot$ increase with temperature in solid matrices, which indicate that during the lifetime of the excited state of the porphyrin moiety[30b,48] the two ends of the linked molecule need to maintain a sufficient degree of vibrotational mobility such that conformations favorable to electron transfer are sampled. It is interesting that in vivo photooxidation of the primary donor P870 of bacterial reaction centers can be carried out at very low temperatures with high quantum yields;[7] hence, the structure of the reaction-center protein apparently does not require vibrotational mobility.

The existing literature on the detailed photophysics and photochemistry of intramolecular electron-transfer reactions is rather sparse, and some important questions remain unanswered:[29] (1) What is the effect of the reduction potential of the acceptor on the efficiency and stability of intramolecular electron transfer? (2) What structural features of the linking chain are most important in facilitating rapid forward electron transfer but slow reverse electron transfer? (3) How will rigid linkages affect the kinetics and mechanisms? (4) How can the quantum yields of stabilized electron transfer be improved? We hope that with further research the answers to some of these questions will be obtained. Subsequent papers will deal with the fluorescence properties[30b] of these compounds and their behavior under nanosecond laser flash photolysis,[49] which shows evidence of much higher quantum yields for transient formation of $P^{+}\cdot Q^{-}\cdot$.

Acknowledgments. We thank Chris Fahrner for technical assistance in performing the low-temperature optical absorption studies. We also thank Dr. John S. Connolly of the Solar Energy Research Institute, Golden, CO, for his valuable comments during the writing of this paper. At our suggestion Dr. T. Shida of Kyoto University, Kyoto, Japan, carried out the measurement of the optical spectrum of 2-methyl-*p*-benzoquinone radical anion. We are grateful to him for providing these useful results. We are grateful to Dr. R. Sealy and Dr. C. C. Felix at the National EPR Center of the Medical College of Wisconsin (NIH Grant RR01008) in Milwaukee for their generous assistance in performing the low-temperature EPR measurements at Q-band on their apparatus. This work was supported financially by a Strategic Grant in Energy to J.R.B. and A.C.W. and an Operating Grant to M.J.S. from the Natural Sciences and Engineering Research Council of Canada and by an Academic Development Fund Equipment Grant to M.J.S. from the University of Western Ontario.

Registry No. PA2AQ, 84426-25-5; PA3AQ, 84445-21-6; PA4AQ, 84426-26-6.

(44) (a) Lexa, D.; Reix, M. *J. Chim. Phys. Phys.-Chim. Biol.* **1974**, *71*, 517–524. (b) Meot-Ner, M.; Adler, A. D. *J. Am. Chem. Soc.* **1975**, *97*, 5107–5111. (c) Gasyna, Z.; Browett, W. R.; Stillman, M. J., unpublished data.

(45) Patel, K. B.; Willson, R. L. *J. Chem. Soc., Faraday Trans. 1* **1973**, 814–825.

(46) Shida, T. (personal communication) has measured the optical spectrum of the methyl-*p*-benzoquinone radical anion in 2-methyltetrahydrofuran at 110 K and found extinction coefficients of 2.85×10^4 (325 nm), 7.8×10^3 (425 nm), and 8.4×10^3 (450 nm). Therefore, the differential extinction coefficient for $Q/Q^{-}\cdot$ at 450 nm is relatively small ($\sim 8 \times 10^3$), and hence it is not surprising that the difference spectrum for $PQ/P^{+}\cdot Q^{-}\cdot$ in Figure 6c appears to be dominated by the $P/P^{+}\cdot$ spectral changes. However, the positive absorbance changes below 400 nm in Figure 6c may be partly correlated with the $Q/Q^{-}\cdot$ difference spectrum.

(47) (a) Wraight, C. A.; Clayton, R. K. *Biochim. Biophys. Acta* **1974**, *333*, 246–260. (b) Also, in vivo there probably exist one or more intermediate electron acceptors which help to mediate the electron transfer process.

(48) Nanosecond flash photolysis studies with optical detection have been carried out in collaboration with Dr J. S. Connolly at the Solar Energy Research Institute. These measurements point strongly to the excited singlet state as the precursor of electron transfer. These results will be reported elsewhere.[49]

(49) Connolly, J. S.; Bolton, J. R.; Marsh, K. L.; Cook, D. R.; Ho, T-F.; Weedon, A. C., paper 3 of this series (to be submitted for publication).